The Astrophysical Journal Letters, 907:L28 (10pp), 2021 February 1 https://doi.org/10.3847/2041-8213/abd8c8

Identification of a Local Sample of Gamma-Ray Bursts Consistent with a Magnetar Giant Flare Origin

E. Burns[1], D. Svinkin[2], K. Hurley[3], Z. Wadiasingh[4,5], M. Negro[6], G. Younes[7,8], R. Hamburg[9], A. Ridnaia[2], D. Cook[10], S. B. Cenko[4,11], R. Aloisi[12,13], G. Ashton[14], M. Baring[15], M. S. Briggs[9], N. Christensen[16], D. Frederiks[2], A. Goldstein[17], C. M. Hui[18], D. L. Kaplan[12], M. M. Kasliwal[19], D. Kocevski[18], O. J. Roberts[17], V. Savchenko[20], A. Tohuvavohu[21], P. Veres[9], and C. A. Wilson-Hodge[18]

[1] Department of Physics & Astronomy, Louisiana State University, Baton Rouge, LA 70803, USA
[2] Ioffe Physical-Technical Institute, Politekhnicheskaya 26, St. Petersburg, 194021, Russia
[3] Space Sciences Laboratory, University of California, 7 Gauss Way, Berkeley, CA 94720-7450, USA
[4] NASA Goddard Space Flight Center, 8800 Greenbelt Road, Greenbelt, MD 20771, USA
[5] Universities Space Research Association, Columbia, MD 21046, USA
[6] University of Maryland, Baltimore County, 1000 Hilltop Circle, Baltimore, MD 21250, USA
[7] Department of Physics, The George Washington University, Washington, DC 20052, USA
[8] Astronomy, Physics and Statistics Institute of Sciences (APSIS), The George Washington University, Washington, DC 20052, USA
[9] Department of Space Science, University of Alabama in Huntsville, Huntsville, AL 35899, USA
[10] IPAC/Caltech, 1200 East California Boulevard, Pasadena, CA 91125, USA
[11] Joint Space-Science Institute, University of Maryland, College Park, MD 20742, USA
[12] University of Wisconsin–Milwaukee, P.O. Box 413, Milwaukee, WI 53201, USA
[13] Department of Astronomy, University of Wisconsin–Madison, 475 North Charter Street, Madison, WI 53706, USA
[14] OzGrav: The ARC Centre of Excellence for Gravitational Wave Discovery, Clayton, VIC 3800, Australia
[15] Department of Physics and Astronomy, Rice University, MS-108, P.O. Box 1892, Houston, TX 77251, USA
[16] Artemis, Université Côte dAzur, Observatoire de la Côte dAzur, CNRS, Nice F-06300, France
[17] Science and Technology Institute, Universities Space Research Association, Huntsville, AL 35805, USA
[18] Astrophysics Office, ST12, NASA/Marshall Space Flight Center, Huntsville, AL 35812, USA
[19] Division of Physics, Mathematics, and Astronomy, California Institute of Technology, Pasadena, CA 91125, USA
[20] Department of Astronomy, University of Geneva, Ch. dEcogia 16, 1290, Versoix, Switzerland
[21] Department of Astronomy & Astrophysics, University of Toronto, 50 St. George Street, Toronto, ON, M5S 3H4, Canada
Received 2020 December 1; revised 2021 January 5; accepted 2021 January 5; published 2021 January 28

Abstract

Cosmological gamma-ray bursts (GRBs) are known to arise from distinct progenitor channels: short GRBs mostly from neutron star mergers and long GRBs from a rare type of core-collapse supernova (CCSN) called collapsars. Highly magnetized neutron stars called magnetars also generate energetic, short-duration gamma-ray transients called magnetar giant flares (MGFs). Three have been observed from the Milky Way and its satellite galaxies, and they have long been suspected to constitute a third class of extragalactic GRBs. We report the unambiguous identification of a distinct population of four local (<5 Mpc) short GRBs, adding GRB 070222 to previously discussed events. While identified solely based on alignment with nearby star-forming galaxies, their rise time and isotropic energy release are independently inconsistent with the larger short GRB population at >99.9% confidence. These properties, the host galaxies, and nondetection in gravitational waves all point to an extragalactic MGF origin. Despite the small sample, the inferred volumetric rates for events above 4×10^{44} erg of $R_{\rm MGF} = 3.8^{+4.0}_{-3.1} \times 10^5\,{\rm Gpc}^{-3}\,{\rm yr}^{-1}$ make MGFs the dominant gamma-ray transient detected from extragalactic sources. As previously suggested, these rates imply that some magnetars produce multiple MGFs, providing a source of repeating GRBs. The rates and host galaxies favor common CCSN as key progenitors of magnetars.

Unified Astronomy Thesaurus concepts: Gamma-ray bursts (629); Magnetars (992); Soft gamma-ray repeaters (1471)

1. Introduction

The histories of gamma-ray bursts (GRBs) and magnetars are intertwined. Short bursts of gamma rays were recorded by the Vela satellites beginning in 1967 (Klebesadel et al. 1973) and were given the phenomenological name GRBs. The InterPlanetary Network (IPN) localized GRB 790305B to the Large Magellanic Cloud (Mazets et al. 1979; Evans et al. 1980). It was unique in being the brightest event seen at Earth, the prompt emission had a long-lasting, exponentially decaying periodic tail (Barat et al. 1979), and additional weaker bursts were localized to the same source (Mazets et al. 1979). Immediately, there were papers investigating whether the main event shared a common origin with other GRBs (Cline et al. 1980; Mazets et al. 1982). It is now known to be the first signal identified from a magnetar.

Key results on the nature of GRBs in the subsequent decades were often proven by population-level statistical analysis before direct "smoking-gun" proof. Perhaps the greatest debate was whether these events had a galactic or an extragalactic origin, with the latter initially disfavored, as it would require intrinsic energetics beyond anything previously known. Proof came first indirectly via statistical studies of the spatial distribution of GRBs (Meegan et al. 1992) and then directly from redshift measurements (Metzger et al. 1997).

Studies of the prompt GRB emission provided strong evidence in favor of two populations (Kouveliotou et al. 1993), with short and long GRBs traditionally separated at 2 s, as measured by the T_{90} parameter. Long GRBs were tied to

broad-line type Ic core-collapse supernovae (CCSNe) called collapsars (Galama et al. 1998). The Neil Gehrels Swift Observatory (Swift) mission enabled successful detections of afterglow from a sample of short GRBs. Circumstantial evidence pointed toward a neutron star merger origin (Eichler et al. 1989; Fong et al. 2015), with direct confirmation that some GRBs arise from binary neutron star mergers coming with GW170817 and GRB 170817A (Abbott et al. 2017).

Yet another debate on the behavior of GRBs is whether or not the sources repeated. This is best explained using modern parlance. Soft gamma-ray repeaters (SGRs) are galactic magnetars named phenomenologically for the weak, recurrent short bursts that first identified them before their physical origin was known. SGR flares are classified as distinct from GRBs and have recently been tied to radio emission similar to the cosmological fast radio bursts (Bochenek et al. 2020). The flare on 1979 March 5 and the subsequent similar events GRB 980827 (Hurley et al. 1999; Mazets et al. 1999b) and GRB 041227 (Palmer et al. 2005; Frederiks et al. 2007a) from magnetars in the Milky Way are referred to as magnetar giant flares (MGFs). The designation for the prompt emission of MGFs often carries the GRB designation, which we use here. GRBs are not thought to repeat as collapsars and neutron star mergers are cataclysmic events. While several galactic magnetars have been observed to produce multiple SGR flares, none have been observed to produce multiple giant flares (though this is not surprising). The historic debate on potential repeating GRBs was likely confounded by magnetar transients before the separation of SGR flares from GRBs.

We here refer to GRBs 790305B, 980827, and 041227 as the known MGF sample. The detection of three from the Milky Way and its satellite galaxies implies a high intrinsic rate on a per-galaxy or volumetric basis. These events should be detectable to extragalactic distances by GRB monitors such as Konus-Wind (Aptekar et al. 1995), Swift-BAT (Barthelmy et al. 2005), and Fermi-GBM (Meegan et al. 2009). However, at these distances, only the immediate bright spike would be detectable, and the event should resemble a short GRB (Hurley et al. 2005). There are two events discussed in previous literature as extragalactic MGF candidates, GRB 051103 (Ofek et al. 2006; Frederiks et al. 2007b; Hurley et al. 2010) and GRB 070201 (Mazets et al. 2008; Ofek et al. 2008), whose chance alignment coincidence was measured to be ∼1% (Svinkin et al. 2015).

There have been population-level searches for additional events, which identified no additional candidates (Popov & Stern 2006; Ofek 2007; Svinkin et al. 2015). However, these studies allow us to constrain the fraction of detected short GRBs that have an MGF origin; Ofek (2007) showed that the rate of galactic events requires this to be >1%, while the lack of additional candidates found in several searches constrains the upper bound to be <8% (Tikhomirova et al. 2010; Svinkin et al. 2015; Mandhai et al. 2018). These studies and their conclusions generally assumed that the brightest MGFs could be detectable to tens of megaparsecs.

Recently, GRB 200415A was identified as the third and likeliest extragalactic MGF (Svinkin et al. 2021). In this work, we perform a new population-level search utilizing the largest GRB sample and new galaxy catalogs that are both more complete and provide additional information, and we develop a new formalism to determine if we can prove that extragalactic MGFs contribute to the observed GRB population. Section 2.4 details the search formalism that identifies four nearby events, identifying an additional extragalactic candidate. The progenitors of our identified sample are investigated in Section 3, the implications of which are discussed in Section 4. We conclude with discussions in Section 5.

2. Local GRBs

The "smoking-gun" evidence of an MGF is the long periodic tails, which are modulated by the rotation period of the neutron star (Hurley et al. 1999) and also show quasi-periodic oscillations related to the modes of the neutron star itself (Barat et al. 1983; Israel et al. 2005; Strohmayer & Watts 2005; Watts & Strohmayer 2006). However, these signatures are not unambiguously identifiable at extragalactic distances with existing instruments. As such, we follow prior population-level searches and focus on spatial information; if a well-localized short GRB is an MGF, it should occur within ∼50 Mpc and be consistent with a cataloged galaxy. We combine existing GRB and galaxy catalogs to build the most complete set of information from existing literature. For each individual burst, we quantify our belief that it is an MGF from a known galaxy through comparison of two probability distribution functions (PDFs), which are discussed below. These PDFs are generated in HEALPix (Gorski et al. 2005). The resolution of the HEALPix maps is defined by the NSIDE parameter, where the number of total pixels is equal to the square of the NSIDE times 12. The maps were generated with NSIDE = 8192, corresponding to a pixel width of ∼0.′5.

2.1. The GRB Sample

We utilize data from the BATSE instrument on board the Compton Gamma-Ray Observatory (Fishman et al. 1989), Konus-Wind (Aptekar et al. 1995), Swift-BAT (Barthelmy et al. 2005), Fermi-GBM (Meegan et al. 2009), and additional information from the IPN.[22] Triggers from the same events were matched utilizing temporal information for all events and spatial information (Ashton et al. 2018) when available. The total sample contains more than 11,000 GRBs observed, with >1200 short GRBs using the standard 2 s cutoff.

Our burst sample selection requires three things. First, we consider only short GRBs ($T_{90} < 2$ s), where the T_{90} used is the shortest reported by any triggering instrument. Second, we require the bolometric fluence (1 keV–10 MeV) determined from a broadband instrument (Konus, BATSE, or GBM), converting from the instrument-specific ranges as necessary. Intercalibration uncertainties are within 25%. For the trigger times, duration, and spectral properties, we utilized the latest catalog information (Paciesas et al. 1999; Lien et al. 2016; Svinkin et al. 2016; von Kienlin et al. 2020), updated online catalogs,[23] and GCN circulars and performed dedicated analysis when necessary.

Lastly, we require well-localized GRBs constructed from all available information. For BATSE localization, we utilize the latest catalogs (Goldstein et al. 2013) and apply the largest systematic error (Briggs et al. 1999). Swift-BAT positions are taken from the updated Swift-BAT Catalog,[24] and Swift-XRT localizations are utilized when available.[25] Fermi-GBM

[22] ssl.berkeley.edu/ipn3/index.html
[23] http://www.ioffe.ru/LEA/shortGRBs/Current/index.html
[24] https://swift.gsfc.nasa.gov/results/batgrbcat/index.html
[25] https://swift.gsfc.nasa.gov/archive/grb_table/

localizations are quasi-circular and were generated using the latest methods (Goldstein et al. 2020) for all bursts.

Konus localizations are an ecliptic band, which are summarized in the IPN catalogs. The IPN compiles localization information for GRBs, including the timing annuli derived from the relative arrival times of gamma rays at distant spacecraft. The information used here is from the IPN localizations of Konus short GRBs through 2020 (Pal'Shin et al. 2013) and the IPN list kept up to date online.[26] Additional IPN localizations were compiled for more than 100 additional short GRBs for this work, which were added to the online table. The location information, including systematic error, from the autonomous localizations, timing annuli, and Earth occultation selections are converted to the HEALpix format using the GBM Data Tools.[27] These independent PDFs are combined into a final PDF referred to as $P^{\rm GRB}$.

The localization threshold is set to a 90% confidence area <4.125 deg^2 when including systematic error. This value is chosen because it is 1/10,000 the area of the sky, comparable to the sum of the angular size of galaxies (as defined in the following section) within 200 Mpc, and between previously used thresholds (Svinkin et al. 2015). With the bolometric fluence measure requirement and the removal of bursts with known redshift (Lien et al. 2016) beyond the distance where the event may be a detected MGF, we are left with a sample of 250 short GRBs. We do not apply more stringent cuts on spectral or temporal information at this stage, as the relevant parameters are not uniformly reported in GRB catalogs.

2.2. The Galaxy Sample

For the galaxies considered in this work, we require the position (R.A., decl., distance), angular extent (if nonnegligible at our spatial resolution; they are represented here as ellipses), and current star formation rate (SFR). The $z=0$ Multi-wavelength Galaxy Synthesis (z0MGS) Catalog (Leroy et al. 2019) combines the ultraviolet observations from the Galaxy Evolution Explorer (Morrissey et al. 2007) with the infrared observations of the Wide-field Infrared Survey Explorer (WISE; Wright et al. 2010) to uniformly measure gas and dust for galaxies within approximately 50 Mpc. As a result, for galaxies contained in this catalog, these measures of the distance and SFR are our default values. The angular size of galaxies is represented as an ellipse when the data allow or a circle when the axial ratio is not known. Angular extent is taken from the input catalogs but is generally the Holmberg isophote, i.e., where the B-band brightness is 26.5 mag arcsec^2.

The Census of the Local Universe (CLU) Catalog (Cook et al. 2019) aims to provide the most complete catalog of galaxies out to 200 Mpc. We use the CLU measures of distance and SFR when they are not provided by z0MGS, and we use the CLU measures for angular size (which are not provided by z0MGS). When missing, we add position angle information from HyperLEDA (Paturel et al. 2003). The SFR measures of these two catalogs correct for internal extinction using WISE4/far-UV luminosities. To ensure completeness within <10 Mpc, we supplement these two catalogs with the Local Volume Galaxy (LVG) Catalog (Karachentsev & Kaisina 2013). The three catalogs are matched by name, with help from the NASA/IPAC Extragalactic Database (NED),[28] and position information.

We consider galaxies between 0.5 Mpc (excluding the Milky Way and its satellite galaxies) and 200 Mpc (beyond where MGFs can be detected), which leaves more than 100,000 galaxies. The SFR is a key parameter in our method, and our inferences also rely on scaling the properties of our host galaxy. The Milky Way SFR used here is $1.65\pm0.19\,M_\odot\,{\rm yr}^{-1}$ (Licquia & Newman 2015). We specify the SFR for NGC 3256, which was identified in Popov & Stern (2006) as being a likely source of detectable extragalactic MGFs. We searched the literature for values of the active SFR in this galaxy and took the value of $\sim$36 $M_\odot\,{\rm yr}^{-1}$ from Lehmer et al. (2015), which is inferred using UV information and is among the middle reported values.

2.3. MGF Spatial Distribution

We seek an all-sky PDF, $P^{\rm MGF}$, representing the probability that a given position will produce a MGF with a particular fluence at Earth. Note that this is determined by the fluence of each burst considered but is constructed independently of the location of the burst itself, $P^{\rm GRB}$. The comparison of the two PDFs generated for each burst quantifies the likelihood that a given short GRB has an MGF origin, which is performed in the next section. This section details the burst-specific construction of $P^{\rm MGF}$.

If a given burst has an MGF origin it should arise from a cataloged galaxy and its intrinsic energetics should fall into the expected range. To construct this, we compute a weight for each galaxy representing how likely it is to have produced the observed fluence for the burst under consideration. This weight has two components: a linear weighting with SFR and a more complex weighting that compares the inferred intrinsic energetics (determined by the burst fluence and potential host galaxy distance) against an assumed PDF.

Magnetars are expected to be able to produce MGFs only for a short period of time (approximately 10 kyr; Beniamini et al. 2019), tying the predicted rate of MGFs to the rate of their formation. The rate of CCSNe can be inferred from the SFR, since the lifetimes of stars that undergo core collapse are much shorter than the timescale probed by the SFR tracers (Botticella et al. 2012). Under the assumption that the dominant formation channel for magnetars is CCSNe (which is explored in Section 4), we can infer the rate of MGFs from a galaxy from its SFR. Thus, each galaxy is linearly weighted with SFR. We use the far-UV measure of SFR (Lee et al. 2010) when available, as it should track massive stars likely to undergo core collapse; otherwise, we use the Hα measure (Kennicutt 1998) scaled by the average difference from galaxies with both measures to account for the lack of dust correction in the LVG catalog.

Next, we can determine the total isotropic-equivalent energetics of a potential burst–galaxy pair as $E_{\rm iso}=4\pi d^2 S$, where S is the burst fluence and d is the distance to the potential host. This value can be compared to an assumed intrinsic energetics PDF to determine how likely the event is to be an MGF. For example, a particularly high fluence short GRB spatially aligned with a distant galaxy would require an intrinsic energetics far beyond what has been observed in the galactic MGFs, excluding an MGF origin. We note that some

[26] http://www.ssl.berkeley.edu/ipn3/

[27] https://fermi.gsfc.nasa.gov/ssc/data/analysis/gbm/gbm_data_tools/gdt-docs/

[28] https://ned.ipac.caltech.edu/

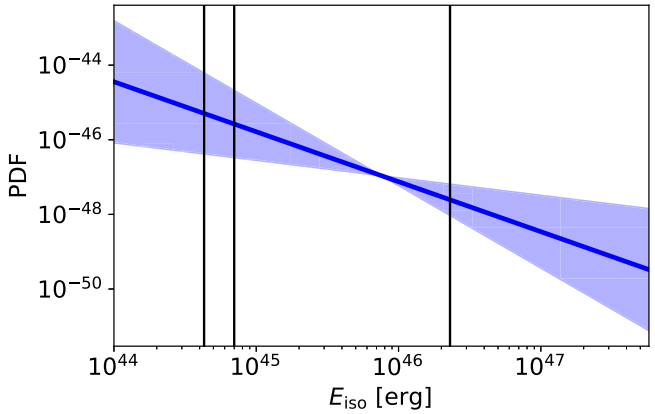

Figure 1. Initial assumed MGF energetics distribution, with $E_{\rm iso,\ min}$ and $E_{\rm iso,\ max}$ set to the x-axis boundaries. The PDF form is $(1-\alpha)E_{\rm iso}^{-\alpha}/(E_{\rm max}^{1-\alpha}-E_{\rm min}^{1-\alpha})$. As described in the text, $\alpha = 1.3 \pm 0.9$ (at 90% confidence). The three $E_{\rm iso}$ values from the known MGFs used to constrain the slope are shown as black vertical lines.

studies utilize the peak luminosity $L_{\rm iso}^{\rm Max}$, but we work with an $E_{\rm iso}$ distribution, as there is stronger theoretical guidance on the maximum total energy that can be released (related to the magnetic fields of the magnetar) than on the timescale on which it is released.

We now construct an informed intrinsic energetics function, assuming a power-law distribution with an assumed minimum and maximum value, which is similar to the behavior of lower-energy magnetar flares (Cheng et al. 1996). Our method bypasses the need for an assumed detection threshold, which is difficult to quantify when considering many instruments over 30 yr. The assumed and inferred values are reported below, with the initially determined distribution shown in Figure 1.

The slope of a power law can be determined via maximum likelihood, independent of an assumed maximum value, as

$$\alpha = 1 + n\left[\sum_{i=1}^{n} \ln\left(\frac{E_{\rm iso,\ i}}{E_{\rm iso,min}}\right)\right]^{-1},\ \sigma_\alpha = \frac{\alpha - 1}{\sqrt{n}} + O(n^{-1}), \quad (1)$$

where the sum is over the observed $E_{\rm iso}$ and $E_{\rm iso,min}$ is the lowest considered value (Newman 2005; Bauke 2007). We set $E_{\rm iso,min}$ as 1.0×10^{44} erg, which is a factor of a few below the lowest value measured in a known MGF, as shown in Table 1, but above the brightest SGR flare that lacked the periodic tail emission (Mazets et al. 1999a). Iterating over the $E_{\rm iso}$ values of the known MGFs (GRBs 790305B, 090827, and 041227) gives $\alpha = 1.3 \pm 0.9$ at 90% confidence, where we have included the $O(n^{-1})$ error contribution. In order to minimize the required computation, we assume the centroid ($\alpha = 1.3$) in what follows; the effect of this assumption on our results is discussed in the closing paragraph of this section.

There must be a physical maximum energy for an MGF, which should be related to the total magnetic energy. This is supported by the lack of detection of more energetic events otherwise consistent with an MGF origin. The highest $E_{\rm iso}$ observed for a known MGF is 2.3×10^{46} erg, which comes from the magnetar with the highest reported magnetic field at the surface of 2.0×10^{15} G (Olausen & Kaspi 2014). We note that this reported value is approximately three times larger than the dipolar spin-down inferred magnetic field value of 7×10^{14} G (Younes et al. 2017), but we have confirmed that this does not affect our results. To determine an $E_{\rm iso,\ max}$ for our search, we assume a dipole field, where the available energy scales as B^2, and a nominal maximum magnetic field strength of $\sim 1.0 \times 10^{16}$ G. This gives $E_{\rm iso,\ max} = 2.3 \times 10^{46}\,{\rm erg} \times (1.0 \times 10^{16}\,{\rm G}/2.0 \times 10^{15}\,{\rm G})^2 = 5.75 \times 10^{47}$ erg.

This allows us to determine the burst-specific two-component weight for each of the >100,000 galaxies in our sample, which are weighted linearly by SFR multiplied by the value of the $E_{\rm iso}$ PDF for the inferred energetics considering the burst fluence and galaxy distance. The sum of the galaxy weights is normalized to unity. Then, $P^{\rm MGF}$ is built by placing the calculated weights at the position of the host galaxy. If the angular diameter of the galaxy is larger than the effective resolution of our discrete sky representation ($\sim$arcmin^2), then its weight is uniformly distributed over its angular extent.

2.4. The Search

For each of the 250 short GRBs in our sample, we generate $P^{\rm GRB}$ from the observations of the GRB and $P^{\rm MGF}$ from theoretically motivated expectations. We quantify the likelihood that a given GRB has an MGF origin using $\Omega = 4\pi \sum_i P_i^{\rm GRB} P_i^{\rm MGF}/A_i$, where $\rm P_i^{GRB}$ and $\rm P_i^{MGF}$ indicate the probability for each PDF in the ith sky region, which has area A_i (Ashton et al. 2018).

Significance is determined by the empirical false-alarm method (e.g., Messick et al. 2017) with Ω as our ranking statistic. Our backgrounds are generated by simulating different galaxy distributions. Each iteration is generated by uniform rotation of the 2D (R.A., decl.) positions of the galaxies in our sample, which maintains the distance and SFR distributions, as well as local structure. Population-level confidence intervals created through comparison of each rotation against our full GRB sample with results are shown in Figure 2. At three and four events, the short GRB sample has an excess surpassing 5σ discovery significance, with individual significance values of the four bursts between 1.2×10^{-4} and 4.9×10^{-6}, as given in Table 1.

Three of the four are discussed in the literature as extragalactic MGF candidates. The Konus-Wind lightcurves are shown in Figure 3. The GRB 070201 has the least robust association with a nearby galaxy; however, the localization is comparatively large ($\sim$10$\times$ the other events), and M31 has the largest angular size of any galaxy in our sample, together lowering Ω even for real associations. We confirm this by checking GRB 790305B with the Large Magellanic Cloud (Evans et al. 1980; Cline et al. 1982), which has an even larger angular extent than M31, giving $\Omega = 500$.

We perform a number of sanity checks to ensure our assumptions do not significantly affect our results. The search we run assumes the centroid $\alpha = 1.3$ value; however, we have confirmed that running the search at the 90% confidence interval bounds ($\alpha = 0.5$, 2.2) identifies the same four bursts as significant outliers and does not identify other candidates. Running the search at greater NSIDE affects our Ω values by <10%. Rerunning the search where the linear SFR weighting is altered to the stellar mass results in identification of the same galaxies but with generally lower Ω values. Running with a specific SFR returns similar results. Together, these suggest a progenitor that tracks SFR. Our results are insensitive to the assumed $E_{\rm iso,\ min}$, so long as we do not exclude known events, as events of this strength are not detected far into the universe. There are a few events with $\Omega > 1$ that are either excluded as

Table 1
A Summary of the MGF Sample

MGF Event	Known 790305B	980827	041227	Extragalactic 200415A	070222	051103	070201
Origin							
False-alarm rate	0	0	0	4.9×10^{-6}	7.8×10^{-6}	1.5×10^{-5}	1.2×10^{-4}
BNS excl. (Mpc)					6.7	5.2	3.5
Galaxy Properties							
Catalog name	LMC	MW	MW	NGC 253	M83	M82	M31
Distance (Mpc)	0.054	0.0125	0.0087	3.5	4.5	3.7	0.78
SFR ($M_\odot$ yr^{-1})	0.56	1.65	1.65	4.9	4.2	7.1	0.4
GRB Properties							
Duration (s)	<0.25	<1.0	<0.2	0.100	0.038	0.138	0.010
Rise time (ms)	~2	~4	~1	2	4	2	24
$L_{\rm iso}^{\rm max}$ (10^{46} erg s^{-1})	0.65	2.3	35	140	40	180	12
$E_{\rm iso}$ (10^{45} erg)	0.7	0.43	23	13	6.2	53	1.6
Index			−0.7	0.0	−1.0	−0.2	−0.6
$E_{\rm peak}$ (keV)	500	1200	850	1080	1290	2150	280

Note. The significance for extragalactic events is from this text. Here BNS excl. refers to the neutron star merger exclusion distances from LIGO, LMC refers to the Large Magellanic Cloud, and MW refers to the Milky Way. Individual significance is determined by comparison of the individual Ω against the full background sample. Distances for the known magnetars come from Olausen & Kaspi (2014); extragalactic distances are taken from the host galaxy values (which have minor variations with our catalog values). The GRB parameters include $E_{\rm peak}$ as the energy of peak output and index as the low-energy power law from the spectral fit, and the rest are discussed in the text. The GRB measures for the galactic events are from the literature; GRB measures for extragalactic events are all measured from Konus-Wind data.

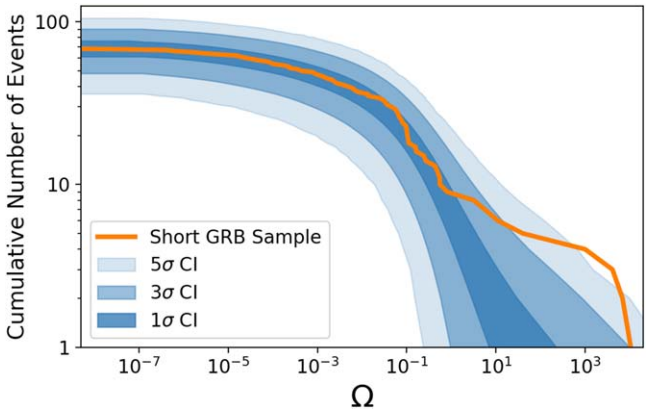

Figure 2. Discovery of a local but extragalactic population of GRBs. Here Ω is a statistic that ranks how believable it is that the event is an extragalactic MGF, with values for the true population shown in orange. The background confidence intervals at 1σ, 3σ, and 5σ are shown in blue. The four most significant events together surpass 5σ discovery significance.

events of interest for our MGF search or insignificant given our sample. Lastly, significantly raising the assumed $E_{\rm iso,\ max}$ marginally identifies GRB 100216A ($\Omega = 10$), which indeed has a potential host galaxy within 200 Mpc (Perley et al. 2010), which is inconsistent with expectations for MGFs.

3. Progenitor Investigations

To determine the origin of these four bursts, we first determine if the known GRB progenitors are compatible. Collapsars power long GRBs with durations $\gtrsim$2 s and are followed immediately by afterglow and then broad-line type Ic supernovae. This origin is excluded, as all four events have durations of 0.1 s or less. Additionally, no subsequent supernovae were reported in any case (Li et al. 2011b; though see Gehrels et al. 2006; Grupe et al. 2007). A neutron star merger origin is excluded by LIGO nondetections in gravitational waves for three of the four events (Abbott et al. 2008; Abadie et al. 2012; Aasi et al. 2014), but observations are insufficiently sensitive to inform on the origin of GRB 200415A. One may consider whether off-axis GRBs could explain these events. The best-known such event is GRB 170817A, where the duration was longer and spectrum softer than the bulk of the short GRB population, which is inconsistent with the prompt emission from these four local events. Further, the rates of these local events (discussed in the following section) are orders of magnitude higher than cosmological GRBs (Siegel et al. 2019), even considering events that are oriented away from Earth.

To determine the progenitors of these events, we follow the historical procedure, where we begin by population comparison of prompt emission parameters. The only additional potential progenitors for extragalactic GRBs commonly discussed in the literature are MGFs, where, contrary to the works that identified the two confirmed progenitors, we have the advantage of observations of galactic events, which are summarized in Table 1. The parameters relevant for only the main peak of the flare that appear distinct from cosmological GRBs are the rise time and intrinsic energetics. Figure 4 contains the population comparison of these parameters.

First, MGFs have rise times of order a few milliseconds, far shorter than most cosmological short GRBs (Hakkila et al. 2018). Rise times are not reported in most GRB catalogs. As a proxy for the rise time, we define the time to peak as the time from the start of the emission to the beginning of the peak 2 ms counts interval. An Anderson–Darling k-sample test against 75 bright Konus short GRBs (~15% brightest bursts detected by Konus between 1994 and 2020) rejects the null hypothesis that

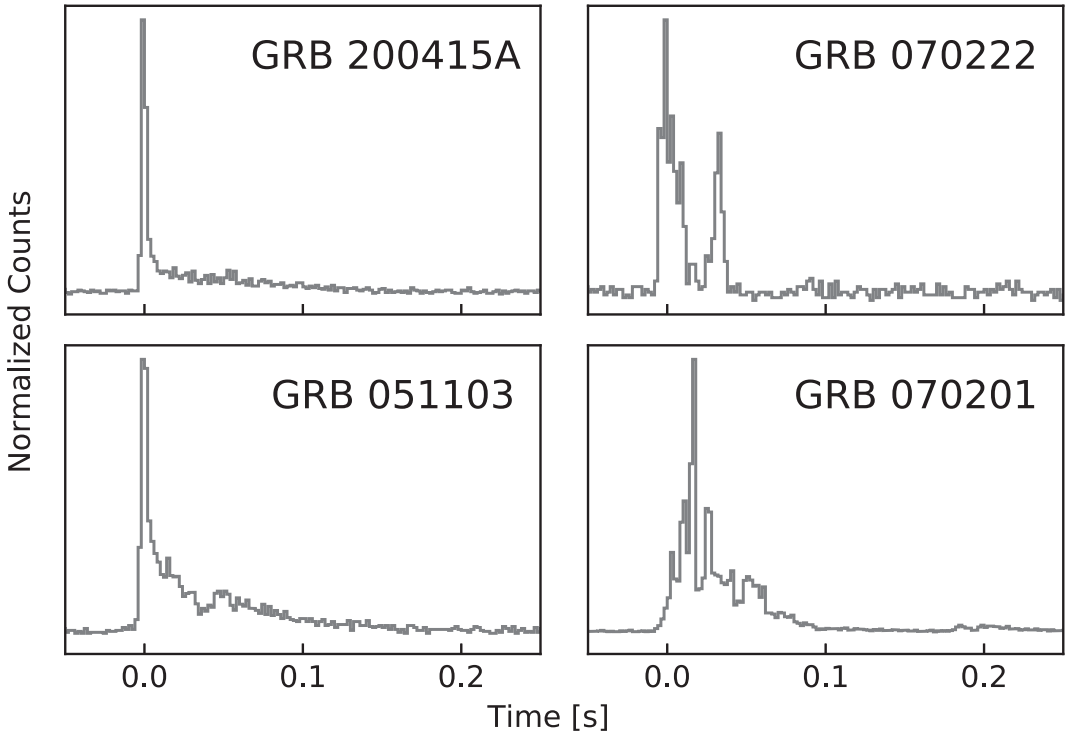

Figure 3. Lightcurves of the candidate extragalactic MGFs in order of significance from Table 1. These are from Konus-Wind and plotted with 2 ms resolution (Frederiks et al. 2007b; Mazets et al. 2008; Svinkin et al. 2021), with GRB 070222 reported here for the first time. While GRBs 200415A and 051103 are strikingly similar (Svinkin et al. 2021) and GRB 070201 is broadly consistent with a single emission episode, GRB 070222 has two temporally and spectrally distinct pulses (see Appendix B), suggesting varied behavior.

they are drawn from the same population at >99.9% confidence.

Second, MGF $E_{\rm iso}$ values are orders of magnitude fainter than cosmological GRBs, where only the unusual GRB 170817A (Abbott et al. 2017) is comparable. This parameter depends on the distance to the source, which is not directly observable from prompt emission. For some cosmological GRBs, the direct distance (redshift) determination is made from follow-up observations. However, for most short GRBs, the distance is determined by first robustly associating the short GRB with an aligned or nearly aligned host galaxy and then determining the distance to the host (Fong et al. 2015). We adapt this last approach for MGFs to enable the use of larger prompt emission localizations and expected host galaxy properties. For each GRB and potential host galaxy, we calculate $\Omega_{\rm host} = 4\pi\sum_i P_i^{\rm GRB} P_i^{\rm host}/A_i$, with $P^{\rm host}$ the weighted spatial distribution of that galaxy. Each GRB has only a single likely host, providing a robust association. In the literature, GRB 051103 has been discussed as belonging to the M81 Group of galaxies (Frederiks et al. 2007b), which is dominated by the interacting galaxies M81 and M82. Our galaxy catalog selection and method assign the burst to M82.

The inferred $E_{\rm iso}$ values for each extragalatic MGF candidate are given in Table 1. For the population comparison, we add the $E_{\rm iso}$ distribution of GBM short GRBs (Abbott et al. 2017) to the sample of Konus bursts with measured redshift (Tsvetkova et al. 2017). Together, these give 23 short GRBs with $E_{\rm iso}$ determined by a broadband instrument, which is the largest such sample to date. The extragalactic MGFs are clearly inconsistent with the broader population, rejecting the null hypothesis at >99.9% confidence.

Host galaxy studies of GRBs have been key in determining prior progenitor channels (e.g., Fong et al. 2015). As discussed in the design of our method, MGFs are expected to arise in star-forming galaxies or regions. Within our maximal detection distance for these bright events, the galaxies with the highest SFR are M82, M83, NGC 253, and NGC 4945 (Mattila et al. 2012). GRB 051103 is associated with M82 by our method or consistent with star-forming knots on the outskirts of M81 (Ofek et al. 2006), GRB 070222 with M83, and GRB 200415A with the star-forming core of NGC 253 (Svinkin et al. 2021). GRB 790305B is associated with the star-forming Large Magellanic Cloud. This is consistent with a massive-star progenitor, as expected for an MGF origin.

Individually, GRBs 200415A and 051103 are the most robust identifications of extragalactic MGFs based on our significance assessment and the results of partner analyses including lightcurve morphology and submillisecond variation of the prompt emission (Roberts et al. 2021; Svinkin et al. 2021). Newly identified is GRB 070222, which is in-class with key properties of MGFs. However, it has two distinct but overlapping pulses, which is not known to occur from galactic events. This requires either a broader morphology of MGFs, a distinct and unknown origin, or a 1 in 100,000 chance alignment (Table 1). However, given the range of (quasi) periodic oscillations seen from magnetar emission, such a morphology is not necessarily surprising.

To summarize the observational case for an MGF origin: these events localize to the nearby universe, particularly to star-forming regions or galaxies. The prompt emission is inconsistent with a collapsar origin, and gravitational wave observations exclude a compact merger involving neutron stars and/or black holes. The event rates, quantified below, are in excess of the majority of energetic astrophysical transients but consistent with predictions from the known MGFs. The properties of the prompt emission are distinct from the larger

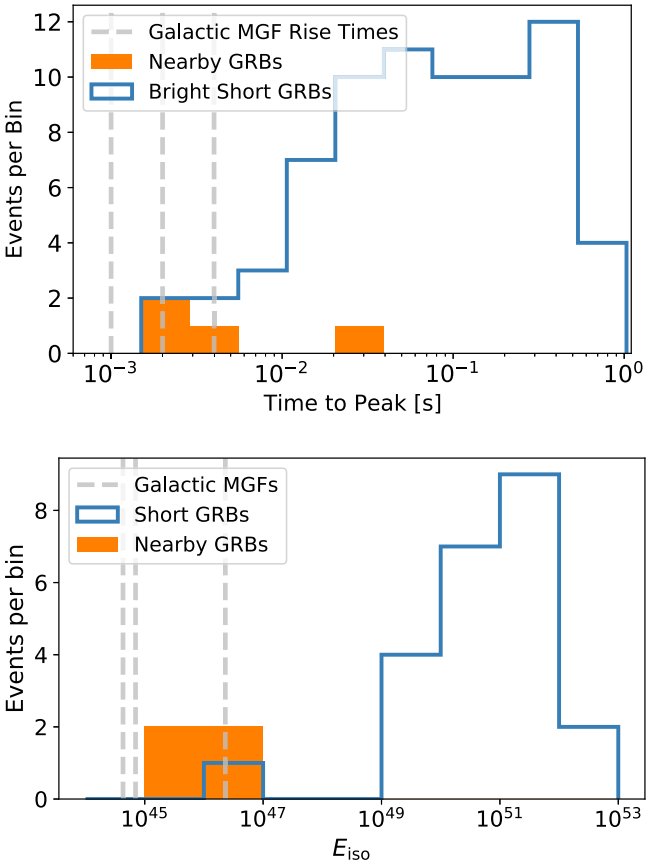

Figure 4. Key parameter comparison of the extragalactic MGF candidates against the wider short GRB population and known MGFs. The top panel shows the time to peak Konus distributions, and the bottom panel shows the E_{iso} distributions. The only comparable E_{iso} value for a burst from a neutron star merger is the off-axis GRB 170817A.

short GRB population but again consistent with the properties from the known MGFs. There is additional evidence for individual events in partner analyses. We conclude that we have confirmed a sample of extragalactic MGFs that match prior predictions on detection rates and properties from both theoretical and observational studies.

A remaining question is, why have we not identified MGFs to greater distances? Previously, MGFs were thought to be detectable to tens of megaparsecs. The spectra of the initial pulse of GRBs 200415A, 051103, and GRB 070222 are particularly spectrally hard, with a shallow spectral index and high peak energies, which is consistent with GRB 041227 (Frederiks et al. 2007a). Assuming a cutoff power-law spectrum for bright MGFs with a low-energy spectral index of ≈0.0 and peak energies of ≈1.5 MeV produces only 15%–20% of the photons in the nominal triggering energy range of 50–300 keV, as compared to a typical short GRB (assuming an index of 0.4 and peak energy of 0.6 MeV; Goldstein et al. 2017). The GRB monitors are triggered by photon counts, which suggests that the harder spectrum reduces the detectable distance by a factor of ∼5 and therefore the volume by a factor of more than 100. Instrument-specific comments are given in Appendix A. Further, there is a local overdensity within ∼5 Mpc of CCSNe (Mattila et al. 2012), which provides an additional explanation of detections within this range and the lack of detections beyond it.

4. Inferences

We now proceed to make population-level inferences utilizing the three known MGFs and treating all four of our events as extragalactic MGFs.

4.1. Intrinsic Energetics Distribution

The power-law distribution of the energetics of normal SGR flares gave hints of the physical process that produces them (Cheng et al. 1996). Thus, it is interesting to measure the slope of the E_{iso} distribution for MGFs. We assign our search volume and detection threshold by empirical means, selecting 2.0×10^{-6} erg cm^{-2} for the IPN and a maximal detection distance of ∼5 Mpc. We further restrict our sample to the past 27 yr, where we have sufficient sensitivity to extragalactic events, leaving the six most recent bursts (excluding GRB 790305B).

We assume the same power-law functional form for the E_{iso} PDF as our search method; however, we cannot utilize the maximum-likelihood estimate because it requires the assumption that the observed sample is complete, which is not true for MGFs at extragalactic distances. Instead, we simulate a large number of extragalactic MGFs by drawing E_{iso} from PDFs over a range of α values, assigning them to specific host galaxies weighted by their SFR, and setting the event distance as the host galaxy distance. Events that would be detected are those where the sampled E_{iso} and distance produce a flux greater than our detection threshold. Here $E_{iso,\,min} = 3.7 \times 10^{44}$ erg is determined by sampling the Kolmogorov–Smirnov test statistic value over a range of viable options (Bauke 2007). Then, we calculate an Anderson–Darling k-sample value for a range of potentially viable α values. We take the 5% rejection values as the bounds on a 90% confidence interval and determine the mean assuming a symmetric Gaussian distribution, giving $\alpha = 1.7 \pm 0.4$. We note that this is consistent with the reported slope values of 5/3 (Cheng et al. 1996) and 1.9 (Götz et al. 2006) recurrent flares from galactic SGRs.

4.2. Rates

Utilizing the same sample and selection as above, we can constrain the intrinsic volumetric rate of MGFs. The dominant sources of uncertainty are the Poisson uncertainty and the imprecisely known sample completeness. The latter is limited by the uncertainty on the power-law index of the intrinsic energetics function, where for a steep index, the majority of events will be missed (with most events below 1.0×10^{45} erg missed in our sample volume), and for a shallow index, most events are recovered. The α distribution is taken as a Gaussian. The SFR within 5 Mpc is 35.5 $M_\odot$ yr^{-1}, which is scaled to a volumetric rate by considering the total SFR within 50 Mpc, which is ∼4000 $M_\odot$ yr^{-1} from our galaxy sample. We infer a volumetric rate of $R_{MGF} = 3.8^{+4.0}_{-3.1} \times 10^5$ Gpc^{-3} yr^{-1}.

4.3. Magnetar Formation Channel

Magnetars may be generated in a variety of events, including common CCSNe, low-mass mergers (Price & Rosswog 2006), a rare evolution of white dwarfs (Dessart et al. 2007), or a rare subtype of CCSN such as collapsars or superluminous supernovae (Nicholl et al. 2017). Each of these is consistent with the observed association of magnetars with supernova remnants (Beniamini et al. 2019). Low-mass merger events

have long inspiral times and should track total stellar mass rather than the current SFR, which is disfavored given our model preference for SFR over stellar mass and the discovery of the first MGF from the Large Magellanic Cloud. A CCSN origin would arise from regions with high rates of star formation. This is consistent with our observations and bolstered by both the lack of detections beyond 5 Mpc due to the local SFR overdensity and the detection of GRB 790305B from the low-mass, star-forming Large Magellanic Cloud. The host galaxies of our extragalactic sample and the Milky Way itself have larger mass and higher metallicity than is typically seen in hosts of collapsars or superluminous supernovae (Taggart & Perley 2019). Therefore, the types of host galaxies favor common CCSNe as the dominant formation channel of magnetars.

Additional support for this conclusion is provided from the event rates. We can relate our inferred MGF rates to progenitor formation rates as $R_{\rm MGF} = R_{\rm event} f_M \tau_{\rm active} r_{\rm MGF/M}$ (Tendulkar et al. 2016), where $R_{\rm event}$ is the rate of events that may form magnetars, f_M is the fraction that successfully forms magnetars, $\tau_{\rm active}$ is the timescale on which magnetars can produce MGFs, and $r_{\rm MGF/M}$ is the rate of MGFs per magnetar. We take $\tau_{\rm active} \approx 10^4$ yr, limited by the decay of the magnetic field (Beniamini et al. 2019). Given the incompleteness of our known magnetar sample and lack of understanding as to which magnetars can produce MGFs, we use only the three known to be capable of producing MGFs to estimate an upper bound of $r_{\rm MGF/M} < 0.02$ yr^{-1} magnetar^{-1}. We note that this is significantly weaker than those reported in the literature that consider all known SGRs, being $\sim 1 \times 10^{-4}$ yr SGR^{-1} (e.g., Ofek 2007; Svinkin et al. 2015).

Of the discussed formation channels, only CCSNe are expected to track star-forming regions and have a comparable rate, being 7×10^4 Gpc^{-3} yr^{-1} in the local universe (Li et al. 2011a). A fiducial value of f_M is 0.4 with a 2σ confidence interval of 0.12–1.0 (Beniamini et al. 2019); other estimates range between 0.01 and 0.1 (e.g., Woods & Thompson 2004; Gullón et al. 2015). We require either that some magnetars produce multiple MGFs or that both $f_M \approx 1$ and the true rate of $R_{\rm MGF}$ are near our 95% lower bound. Alternatively, using the CCSN rate and the 95% lower limit on $R_{\rm MGF}$, we can place observational constraints using our results of $f_M > 0.005$, further excluding particularly rare subtypes of and favoring common CCSNe as the dominant formation channel of magnetars.

5. Conclusions

We summarize our conclusions as follows.

1. We have shown that four short GRBs that occurred within ∼5 Mpc are the closest events by an order of magnitude in distance. Our analysis was the first to identify GRB 070222 as a local event.
2. They are inconsistent with a collapsar or neutron star merger origin.
3. Their prompt emission is inconsistent with the properties of cosmological GRBs but consistent with the observations of the known MGFs.
4. They originate from star-forming regions or galaxies, including those with metallicity that prevents collapsars from occurring.
5. All together, this matches expectations for an MGF origin, which appears to produce 4 out of 250 events. This would be ∼2% of detected short GRBs (consistent with the 1%–8% range from the literature; Ofek 2007; Svinkin et al. 2015) or ∼0.3% of all detected GRBs.
6. Modeling the intrinsic energetics distribution of MGFs as a power law constrains the index to be 1.7 ± 0.4.
7. The volumetric rates are $R_{\rm MGF} = 3.8^{+4.0}_{-3.1} \times 10^5$ Gpc^{-3} yr^{-1}.
8. The rates and host galaxies of these events favor CCSNe as the dominant formation channel for magnetars, requiring at least 0.5% of CCSNe to produce magnetars.
9. We estimate the rate of MGFs per magnetar to be $\lesssim 0.02$ yr^{-1}.
10. Our results suggest that some magnetars produce multiple MGFs; this would be the first known source of repeating GRBs.
11. GRB 070222 suggests that MGFs can have multiple pulses.
12. The MGFs may not be detectable to tens of megaparsecs with existing instruments due to their spectral hardness.

Our analysis suggests that additional extragalactic MGFs may be identified with improved analysis, but "smoking-gun" confirmation likely requires future instruments. The inferred rates are sufficiently high that they may contribute to the stochastic background of gravitational waves. This, along with the recent observations of a fast radio burst to lower-energy gamma-ray flares from magnetars (Bochenek et al. 2020; Li et al. 2020; Marcote et al. 2020; Ridnaia et al. 2020), suggests that the coming years will bring new insights into the physics and emission of magnetars.

N.C. is supported by NSF grant PHY-1806990. The Fermi-GBM Collaboration acknowledges the support of NASA in the United States under grant NNM11AA01A and DRL in Germany. The CLU galaxy list made use of the NASA/IPAC Extragalactic Database (NED), which is funded by the National Aeronautics and Space Administration and operated by the California Institute of Technology, and was supported by the Global Relay of Observatories Watching Transients Happen (GROWTH) project funded by the National Science Foundation under PIRE grant No. 1545949.

Appendix A

We present rough estimates for the maximal detection distance of bright MGFs with representative active instruments. Konus-Wind can detect bright MGFs to ∼13–16 Mpc, based on GRBs 051103 and 200415A (Svinkin et al. 2021). This can be taken as the approximate detection distance of the IPN (Svinkin et al. 2015). The following investigations assume a hard spectrum based on the time-integrated values for the most energetic bursts, with a low-energy spectral index of ≈0.0 and peak energies of ≈1.5 MeV. This has only 15% (20%) of the number of photons over the 15–150 keV (50–300 keV) energy range, reducing the detection distance by ∼5× and thus the volume by >100.

The GBM GRB trigger algorithms cover 50–300 keV, where the short GRB sensitivity is usually quoted over the 64 ms timescale. With the assumed spectral and energetics values, the GBM would have only triggered these onboard algorithms out

to ∼15–20 Mpc. At greater distances, only the peak flux interval would be visible, which would be spectrally harder and reduce this distance. The GBM localizations alone are insufficient to associate events with any specific burst. Ground-based searches for GRBs and terrestrial gamma-ray flashes should be able to recover additional events but may require confirmation on other GRB instruments

The INTEGRAL SPI-ACS and IBIS are especially sensitive to hard and short bursts, and additional extragalactic MGFs have likely triggered the SPI-ACS real-time pipeline in the past. However, SPI-ACS and IBIS lack the capacity to discriminate extragalactic MGFs from high cosmic-ray effects that appear similar to real events in these instruments. The real-time IBAS pipeline has not been tuned to favor short and hard events. We estimate that SPI-ACS would record sufficient signal from extragalactic MGFs for association with another instrument up to 25–35 Mpc but would only independently report much brighter events out to 15–20 Mpc. The sensitivity of IBIS is close to or better than that of SPI-ACS in about 10% of the sky, and in the majority of directions, IBIS would only yield detectable signal for extragalactic MGF flares out to at most 10 Mpc. However, PICsIT may often be more suitable for triangulation, owing to better time resolution, and can provide some spectral characterization.

Swift/BAT has >500 different rate trigger criteria running in real time on board, continuously sampling and testing trigger timescales from 4 ms up to 64 s, each of which is evaluated for 36 different combinations of energy ranges and focal plane regions. While the BAT detector is sensitive to photons with energies up to 500 keV, the transparency of the lead tiles in the mask above 200 keV limits its imaging energy range (necessary for a successful autonomous trigger) to 15–150 keV. This narrow and low energy range limits the BAT's sensitivity to hard events, such as MGFs, despite its high effective area. Due to the number and complexity of the onboard triggering algorithms, the varying computer load on the BAT CPU, the evolving state of the BAT detector array, and the changing operational choices for trigger vetoes/thresholds, modeling the likelihood of an onboard autonomous trigger is quite difficult. In addition, due to the BAT's high effective area, continuous time-tagged event data cannot be downlinked, making it difficult to assess the relative completeness of the triggering algorithms versus ground searches, though this is partly ameliorated by GUANO (Tohuvavohu et al. 2020). Under the assumed energetics and spectral values, we estimate that as of 2020 (averaging half of the original detector array online), Swift/BAT should reliably trigger on MGFs out to ∼25 Mpc in the highest coded region of its field of view. Ground analyses in the downlinked BAT event data can extend this, but the availability of these data will often depend on an external trigger (e.g., GUANO). We note that operational changes to the BAT onboard triggering thresholds with the goal of increasing sensitivity to extragalactic MGFs and local low-luminosity GRBs have been previously attempted. In 2012, the threshold for a successful trigger from an image was lowered from the usual value of 6.5–5.7, with the condition that triggers in this range had to be localized to within 12′ projected offset from a local cataloged galaxy stored in the BAT onboard catalog. No local GRB-like source was ever identified in this program.

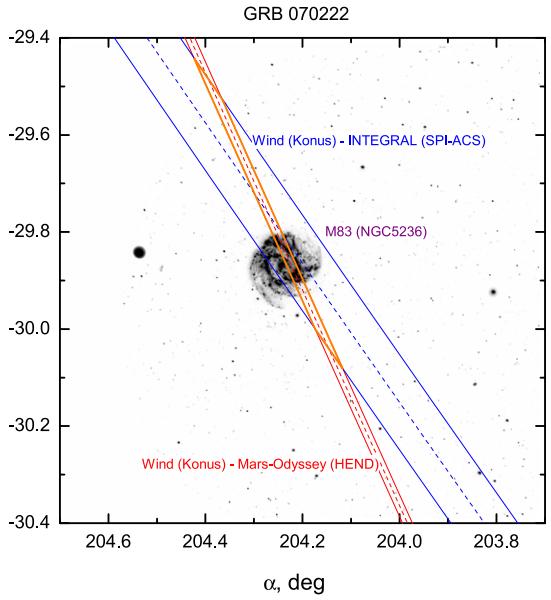

Figure 5. Localization of GRB 070222 compared to the position and angular size of M83.

Table 2
The Time-resolved Analysis of the Two Pulses of GRB 070222

T_{start} (s)	T_{stop} (s)	Index	E_{peak} (keV)	Flux (1×10^{-6} erg s^{-1} cm^{-2})
−0.006	0.012	$0.14^{+0.28}_{-0.24}$	733^{+138}_{-99}	$153.4^{+21.2}_{-16.5}$
0.026	0.038	$-0.27^{+0.48}_{-0.36}$	193^{+25}_{-14}	$24.5^{+3.0}_{-3.0}$

Note. Errors are quoted at 68% confidence. The main pulse is spectrally hard, similar to the time-integrated fits of GRB 200415A and GRB 051103.

Appendix B

As GRB 070222 has not been reported elsewhere, we describe its basic analysis here. The event was detected by Konus-Wind, HEND on Mars Odyssey, and both SPI-ACS and PICsIT on INTEGRAL. Combination of the two best annuli produces a localization with a 90% containment region of 0.004 deg^2. This location and its consistency with M83 are shown in Figure 5.

This burst is distinct from the separate candidates as having two separate pulses. Time-resolved analysis of this burst is summarized in Table 2, while time-integrated analysis is reported in the Second Konus GRB Catalog (Svinkin et al. 2016).

ORCID iDs

E. Burns https://orcid.org/0000-0002-2942-3379
G. Younes https://orcid.org/0000-0002-7991-028X
A. Ridnaia https://orcid.org/0000-0001-9477-5437
D. Cook https://orcid.org/0000-0002-6877-7655
S. B. Cenko https://orcid.org/0000-0003-1673-970X
R. Aloisi https://orcid.org/0000-0003-2822-616X
G. Ashton https://orcid.org/0000-0001-7288-2231
M. Baring https://orcid.org/0000-0003-4433-1365
D. Frederiks https://orcid.org/0000-0002-1153-6340
A. Goldstein https://orcid.org/0000-0002-0587-7042
C. M. Hui https://orcid.org/0000-0002-0468-6025

D. L. Kaplan https://orcid.org/0000-0001-6295-2881
M. M. Kasliwal https://orcid.org/0000-0002-5619-4938
D. Kocevski https://orcid.org/0000-0001-9201-4706
O. J. Roberts https://orcid.org/0000-0002-7150-9061
V. Savchenko https://orcid.org/0000-0001-6353-0808
A. Tohuvavohu https://orcid.org/0000-0002-2810-8764
P. Veres https://orcid.org/0000-0002-2149-9846
C. A. Wilson-Hodge https://orcid.org/0000-0002-8585-0084

References

Aasi, J., Abbott, B., Abbott, R., et al. 2014, PhRvL, 113, 011102
Abadie, J., Abbott, B., Abbott, T., et al. 2012, ApJ, 755, 2
Abbott, B., Abbott, R., Adhikari, R., et al. 2008, ApJ, 681, 1419
Abbott, B. P., Abbott, R., Abbott, T. D., et al. 2017, ApJL, 848, L13
Aptekar, R., Frederiks, D., Golenetskii, S., et al. 1995, SSRv, 71, 265
Ashton, G., Burns, E., Dal Canton, T., et al. 2018, ApJ, 860, 6
Barat, C., Chambon, G., Hurley, K., et al. 1979, A&A, 79, L24
Barat, C., Hayles, R. I., Hurley, K., et al. 1983, A&A, 126, 400
Barthelmy, S. D., Barbier, L. M., Cummings, J. R., et al. 2005, SSRv, 120, 143
Bauke, H. 2007, EPJB, 58, 167
Beniamini, P., Hotokezaka, K., van der Horst, A., & Kouveliotou, C. 2019, MNRAS, 487, 1426
Bochenek, C. D., Ravi, V., Belov, K. V., et al. 2020, arXiv:2005.10828
Botticella, M., Smartt, S., Kennicutt, R., et al. 2012, A&A, 537, A132
Briggs, M. S., Pendleton, G. N., Kippen, R. M., et al. 1999, ApJS, 122, 503
Cheng, B., Epstein, R. I., Guyer, R. A., & Young, A. C. 1996, Natur, 382, 518
Cline, T., Desai, U., Pizzichini, G., et al. 1980, ApJL, 237, L1
Cline, T., Desai, U., Teegarden, B., et al. 1982, ApJL, 255, L45
Cook, D. O., Kasliwal, M. M., Van Sistine, A., et al. 2019, ApJ, 880, 7
Dessart, L., Burrows, A., Livne, E., & Ott, C. D. 2007, ApJ, 669, 585
Eichler, D., Livio, M., Piran, T., & Schramm, D. N. 1989, Natur, 340, 126
Evans, W., Klebesadel, R., Laros, J., et al. 1980, ApJL, 237, L7
Fishman, G., Meegan, C., Wilson, R., et al. 1989, in Proc. GRO Science Workshop, GSFC 2
Fong, W.-f., Berger, E., Margutti, R., & Zauderer, B. A. 2015, ApJ, 815, 102
Frederiks, D. D., Golenetskii, S. V., Palshin, V. D., et al. 2007a, AstL, 33, 1
Frederiks, D. D., Palshin, V. D., Aptekar, R. L., et al. 2007b, AstL, 33, 19
Galama, T. J., Vreeswijk, P., Van Paradijs, J., et al. 1998, Natur, 395, 670
Gehrels, N., Norris, J., Barthelmy, S., et al. 2006, Natur, 444, 1044
Goldstein, A., Fletcher, C., Veres, P., et al. 2020, ApJ, 895, 40
Goldstein, A., Preece, R. D., Mallozzi, R. S., et al. 2013, ApJS, 208, 21
Goldstein, A., Veres, P., Burns, E., et al. 2017, ApJL, 848, L14
Gorski, K. M., Hivon, E., Banday, A. J., et al. 2005, ApJ, 622, 759
Götz, D., Mereghetti, S., Molkov, S., et al. 2006, A&A, 445, 313
Grupe, D., Gronwall, C., Wang, X.-Y., et al. 2007, ApJ, 662, 443
Gullón, M., Pons, J. A., Miralles, J. A., et al. 2015, MNRAS, 454, 615
Hakkila, J., Horváth, I., Hofesmann, E., & Lesage, S. 2018, ApJ, 855, 101
Hurley, K., Boggs, S., Smith, D., et al. 2005, Natur, 434, 1098
Hurley, K., Cline, T., Mazets, E., et al. 1999, Natur, 397, 41
Hurley, K., Rowlinson, A., Bellm, E., et al. 2010, MNRAS, 403, 342
Israel, G., Belloni, T., Stella, L., et al. 2005, ApJL, 628, L53
Karachentsev, I. D., & Kaisina, E. I. 2013, AJ, 146, 46
Kennicutt, R. C., Jr. 1998, ARA&A, 36, 189
Klebesadel, R. W., Strong, I. B., & Olson, R. A. 1973, ApJL, 182, L85
Kouveliotou, C., Meegan, C. A., Fishman, G. J., et al. 1993, ApJL, 413, L101
Lee, J. C., De Paz, A. G., Kennicutt, R. C., Jr., et al. 2010, ApJS, 192, 6
Lehmer, B., Tyler, J., Hornschemeier, A., et al. 2015, ApJ, 806, 126
Leroy, A. K., Sandstrom, K. M., Lang, D., et al. 2019, ApJS, 244, 24
Li, C., Lin, L., Xiong, S., et al. 2020, arXiv:2005.11071
Li, W., Chornock, R., Leaman, J., et al. 2011a, MNRAS, 412, 1473
Li, W., Leaman, J., Chornock, R., et al. 2011b, MNRAS, 412, 1441
Licquia, T. C., & Newman, J. A. 2015, ApJ, 806, 96
Lien, A., Sakamoto, T., Barthelmy, S. D., et al. 2016, ApJ, 829, 7
Mandhai, S., Tanvir, N., Lamb, G., Levan, A., & Tsang, D. 2018, Galax, 6, 130
Marcote, B., Nimmo, K., Hessels, J., et al. 2020, Natur, 577, 190
Mattila, S., Dahlén, T., Efstathiou, A., et al. 2012, ApJ, 756, 111
Mazets, E., Aptekar, R., Butterworth, P., et al. 1999a, ApJL, 519, L151
Mazets, E., Cline, T., Aptekar, R., et al. 1999b, arXiv:astro-ph/9905196
Mazets, E., Golenetskii, S., Gurian, I. A., & Ilinskii, V. 1982, Ap&SS, 84, 173
Mazets, E., Golenetskii, S., Il'Inskii, V., Guryan, Y. A., et al. 1979, Natur, 282, 587
Mazets, E. P., Aptekar, R. L., Cline, T. L., et al. 2008, ApJ, 680, 545
Meegan, C., Fishman, G., Wilson, R., et al. 1992, Natur, 355, 143
Meegan, C., Lichti, G., Bhat, P. N., et al. 2009, ApJ, 702, 791
Messick, C., Blackburn, K., Brady, P., et al. 2017, PhRvD, 95, 042001
Metzger, M., Djorgovski, S., Kulkarni, S., et al. 1997, Natur, 387, 878
Morrissey, P., Conrow, T., Barlow, T. A., et al. 2007, ApJS, 173, 682
Newman, M. E. 2005, ConPh, 46, 323
Nicholl, M., Guillochon, J., & Berger, E. 2017, ApJ, 850, 55
Ofek, E., Muno, M., Quimby, R., et al. 2008, ApJ, 681, 1464
Ofek, E. O. 2007, ApJ, 659, 339
Ofek, E. O., Kulkarni, S., Nakar, E., et al. 2006, ApJ, 652, 507
Olausen, S., & Kaspi, V. 2014, ApJS, 212, 6
Paciesas, W. S., Meegan, C. A., Pendleton, G. N., et al. 1999, ApJS, 122, 465
Palmer, D. M., Barthelmy, S., Gehrels, N., et al. 2005, Natur, 434, 1107
Pal'Shin, V., Hurley, K., Svinkin, D., et al. 2013, ApJS, 207, 38
Paturel, G., Petit, C., Prugniel, P., et al. 2003, A&A, 412, 45
Perley, D. A., Meyers, J., Hsiao, E., et al. 2010, GCN, 10429, 1
Popov, S. B., & Stern, B. 2006, MNRAS, 365, 885
Price, D. J., & Rosswog, S. 2006, Sci, 312, 719
Ridnaia, A., Svinkin, D., Frederiks, D., et al. 2020, arXiv:2005.11178
Roberts, O. J., Veres, P., Baring, M. G., et al. 2021, Natur, 589, 207
Siegel, D. M., Barnes, J., & Metzger, B. D. 2019, Natur, 569, 241
Strohmayer, T. E., & Watts, A. L. 2005, ApJL, 632, L111
Svinkin, D., Frederiks, D., Aptekar, R., et al. 2016, ApJS, 224, 10
Svinkin, D. S., Hurley, K., Aptekar, R. L., Golenetskii, S. V., & Frederiks, D. D. 2015, MNRAS, 447, 1028
Svinkin, D., Frederiks, D., Hurley, K., et al. 2021, Natur, 589, 211
Taggart, K., & Perley, D. 2019, arXiv:1911.09112
Tendulkar, S. P., Kaspi, V. M., & Patel, C. 2016, ApJ, 827, 59
Tikhomirova, Y. Y., Pozanenko, A., & Hurley, K. 2010, AstL, 36, 231
Tohuvavohu, A., Kennea, J. A., DeLaunay, J., et al. 2020, ApJ, 900, 35
Tsvetkova, A., Frederiks, D., Golenetskii, S., et al. 2017, ApJ, 850, 161
von Kienlin, A., Meegan, C., Paciesas, W., et al. 2020, ApJ, 893, 46
Watts, A. L., & Strohmayer, T. E. 2006, ApJL, 637, L117
Woods, P., & Thompson, C. 2004, arXiv:astro-ph/0406133
Wright, E. L., Eisenhardt, P. R., Mainzer, A. K., et al. 2010, AJ, 140, 1868
Younes, G., Baring, M. G., Kouveliotou, C., et al. 2017, ApJ, 851, 17